Heat induces the splicing by IRE1 of a mRNA encoding a transcription factor involved in the unfolded protein response in Arabidopsis

Yan Deng[a,1], Sabrina Humbert[b,1], Jian-Xiang Liu[c], Renu Srivastava[a], Steven J. Rothstein[b], and Stephen H. Howell[a,2]

[a]Plant Sciences Institute, Iowa State University, Ames, IA 50011; [b]Molecular and Cellular Biology Department, University of Guelph, Guelph, ON, Canada N1G 2W1; and [c]State Key Laboratory of Genetic Engineering, Institute of Plant Biology, School of Life Sciences, Fudan University, Shanghai 200433, China

Edited by Maarten J. Chrispeels, University of California at San Diego, La Jolla, CA, and approved March 15, 2011 (received for review February 7, 2011)

Adverse environmental conditions produce endoplasmic reticulum (ER) stress in plants. In response to heat or ER stress agents, *Arabidopsis* seedlings mitigate stress damage by activating ER-associated transcription factors and a RNA splicing factor, IRE1b. IRE1b splices the mRNA-encoding bZIP60, a basic leucine-zipper domain containing transcription factor associated with the unfolded protein response in plants. bZIP60 is required for the up-regulation of *BINDING PROTEIN3* (*BIP3*) in response to ER stress, and loss-of-function mutations in *IRE1b* or point mutations in the splicing site of *bZIP60* mRNA are defective in *BIP3* induction. These findings demonstrate that *bZIP60* in plants is activated by RNA splicing and afford opportunities for monitoring and modulating stress responses in plants.

abiotic stress | heat stress | RNA splicing | signal transduction

Heat and drought tolerance are some of the most complex and important adaptive traits in plants. These stresses are foremost in placing limits on plant productivity worldwide, and tolerance to these stresses are among the most highly sought after traits in crops (1), particularly in the face of climate change.

The unfolded protein response (UPR) in eukaryotes is an ER stress response that activates three different classes of membrane-associated sensor transducers in mammalian cells—activating transcription factor 6 (ATF6), inositol-requiring enzyme-1 (IRE1) and protein kinase RNA (PKR)-like ER kinase. Yeast has only one ER stress transducer, *IRE1*; nonetheless, this factor sets off a massive UPR by triggering the expression of >5% of genes in the yeast genome. Many of these encode chaperones and ER-associated protein degradation components (2). IRE1 in yeast and mammalian cells acts by splicing a messenger RNA encoding a transcription factor that, then in turn, activates the expression of stress response genes (see recent reviews; refs. 3–5). Yeast cells splice an mRNA encoding a transcription factor called Hac1p (6, 7). The unspliced form of the *Hac1* messenger RNA attenuates its own translation, and splicing relieves the translational repression (8).

IRE1-mediated splicing is unconventional because mRNA splicing normally occurs in the nucleus, not in the cytoplasm (9). IRE1 is a type I membrane-spanning protein situated in the ER with its N terminus facing the ER lumen and its C terminus, which possesses catalytic functions, facing the cytosol. IRE1 is regarded as a dual functional enzyme possessing both serine/threonine protein kinase and endoribonuclease activity (10). Upon activation, the IRE1 dimer undergoes autotransphosphorylation in which one monomer phosphorylates the other (11). Through the analysis of the structure of the cytosolic domain of IRE1, Lee et al. (12) found that dimerization brings together the kinase domains in a face-to-face manner that would seemingly facilitate autotransphosphorylation.

Autotransphosphorylation is then thought to open a nucleotide-binding site that, when occupied, produces a conformational change in the cytosolic domain so as to position the ribonuclease domains in a back-to-back dimer configuration. The crystal structure of the cytosolic domain shows two ribonuclease centers symmetrically arrayed. Lee et al. (12) reasoned that the configuration is meaningful to the operation of the enzyme because IRE1 cleaves the *Hac1* mRNA in two places. They proposed that the predicted hairpin loops in the RNA substrate pair in a staggered, antiparallel manner so as to form "kissing" hairpin loops. In such a structure, the projected cleavage sites lie close to the ribonuclease catalytic sites in the cytosolic domain of IRE1.

Mammalian cells have two genes that encode IRE1 (*IRE1a* and *IRE1b*). *IRE1a* is widely expressed in animal tissues, but *IRE1b* is largely restricted to cells of the intestinal epithelium (13). Mammalian IRE1 appears to function in the same way as its yeast counterpart. However, mammalian IRE1 splices *XBP1* mRNA (X-box binding protein), which is not related in sequence to *Hac1* but, nonetheless, encodes a bZIP transcription factor that activates stress response genes (14). IRE1 splicing of *XBP* mRNA produces a frameshift resulting in a protein with a different C terminus. When the unspliced pXBP1(U) and spliced forms pXBP1(S) were overproduced in animal cells, the spliced form, pXBP1(S), strongly transactivated a stress promoter:reporter gene (14). The authors also demonstrated that the C terminus of the spliced form is a potent transcriptional activator when fused to a Gal4 binding domain. Yoshida et al. (15) found that pXBP1(U) complexed with pXBP1(S), and the complex was readily degraded because of a degradation domain in pXBP1(U). Therefore, pXBP1(S) is transcriptionally active, whereas pXBP1(U) appears to be a negative regulator of pXBP1(S). During the early phases of the stress response, ATF6 is activated and, in turn, it up-regulates XBP1. IRE1 is also activated and presumably splices the *XBP1* message to produce an active transcription factor that up-regulates stress gene expression. In the later phase of the stress response, *IRE1* expression is thought to fade, resulting in the production of pXBP1 (U), which shuts down XBP1 action (16).

Arabidopsis has two genes with IRE1-related sequences: *AtIRE1a* (At2g17520, formerly Atire1-2) and *AtIRE1b* (At5g24360, formerly Atire1-1), which were first described by Koizumi et al. (17). They found that IRE1a and -b GFP fusions were located in the perinuclear ER. The genome also encodes a shorter *IRE1*-related sequence, At3g11870, lacking the luminal and transmembrane domain. Koizumi et al. (17) demonstrated functional complementation of the *Arabidopsis* luminal domain (sensor domain) in yeast and that the plant IRE1a has autophosphorylation activity in vitro, but they were unable to demonstrate splicing. Noh et al. (18) attempted, but were unsuccessful, in showing that IRE1a could splice yeast *Hac1* RNA in *Arabidopsis* protoplasts.

Author contributions: Y.D., S.H., J.-X.L., S.J.R., and S.H.H. designed research; Y.D., S.H., and R.S. performed research; Y.D. and S.H. analyzed data; and S.H.H. wrote the paper.

The authors declare no conflict of interest.

This article is a PNAS Direct Submission.

Freely available online through the PNAS open access option.

[1]Y.D. and S.H. contributed equally to this work.

[2]To whom correspondence should be addressed. E-mail: shh@iastate.edu.

This article contains supporting information online at www.pnas.org/lookup/suppl/doi:10.1073/pnas.1102117108/-/DCSupplemental.

UPR has been demonstrated in plants in response to ER stress agents such as dithiotreitol (DTT) and tunicamycin (TM) (19). ER stress activates bZIP transcription factors, AtbZIP17 and -28, members of a small family of membrane-associated bZIP factors in *Arabidopsis* (20, 21). AtbZIP17 and -28 are activated by mechanisms similar to the activation of ATF6 in mammalian cells (20–22). Mammalian ATF6 is activated by liberation from the ER and migration to the Golgi apparatus where its C-terminal, lumen-facing domain is cleaved by S1P and S2P proteases, releasing its N-terminal, cytosol-facing component, which enters the nucleus and up-regulates target genes.

bZIP60 also plays an important role in ER stress responses in *Arabidopsis* through the up-regulation of genes encoding factors that aid in protein folding and degradation (23, 24). In response to stress, bZIP60 appears in an active, truncated form seemingly to have undergone proteolytic processing similar to AtbZIP17 and AtbZIP28 (20–22). However, the mechanism for the presumed proteolysis event is not understood, because the C-terminal tail of bZIP60 does not have a canonical S1P cleavage site and its activation does not require S1P or S2P (23). For these reasons, we considered the possibility that activated forms of bZIP60 might arise by different means, by RNA splicing, in a manner similar to the activation of Hac1 in yeast or XBP1 in mammalian cells.

Results

***Arabidopsis bZIP60* mRNA Is the Target of Splicing.** The target sites for *XBP1* and *Hac1* mRNA splicing are a pair of kissing hairpin loops with three conserved bases in each loop (14, 25). Using a RNA structure prediction program (M-fold; ref. 26), we found that the predicted lowest free energy forms for *bZIP60* mRNA folded into twin kissing loops with bases in each loop similar to the conserved bases in *XBP1* and *Hac1* mRNAs (Fig. S1 and Fig. 1*A*). Based on this structure and the known splice sites in the mammalian and yeast RNAs (14, 25), we predicted that if *bZIP60* mRNA is spliced by an IRE1-like activity, then the splice should remove a 23b segment of RNA from that site.

To determine whether splicing occurs in response to treatment of seedlings with ER stress agents, we employed a RT-PCR assay by using primers flanking the predicted splice site (FP assay, Table S1) to detect the removal of a small segment of RNA (Fig. S2*A*). RNA extracted from untreated seedlings gave rise to a RT-PCR product that migrated as a single band on nondenaturing gels (Fig. 1*B*), whereas RNA from seedlings treated with TM produced two bands (Fig. 1*B*). The bands ran true upon reamplification and were shown by sequencing to be derived from the unspliced and spliced forms of *bZIP60* RNA with the predicted splice sites as indicated (Fig. 1*C*).

Additional RT-PCR assays were developed specific for the unspliced transcripts by using primers that cross the exon-to-intron boundary in the unspliced RNA (SPU assay) or specific for the spliced forms using primers that cross the exon-exon boundary in the spliced RNA (SPS assay; Fig. S2 *A* and *B*). The assays were used to monitor *bZIP60* transcripts in seedlings after treatment with the ER stress agent DTT. Spliced *bZIP60* RNA forms could be detected within 5 min of DTT treatment in the more sensitive SPS assay and appeared to increase in amount progressively during the 2 h of treatment (Fig. 2*A*). The SPU assay, in particular, showed a slight increase in unspliced *bZIP60* transcripts after DTT treatment. (In the FP assay, the level of the unspliced band is at saturation to detect the less abundant spliced band.) We also monitored *BINDING PROTEIN3* (*BIP3*) induction, which substantially depends on *bZIP60* (23) and which lags in the appearance of the spliced *bZIP60* mRNA (Fig. 2*A*).

***Arabidopsis IRE1b* Catalyzes the RNA Splicing Reaction.** *Arabidopsis* has two *IRE1* homologs, *AtIRE1a* and *AtIRE1b* (18). To determine whether one or both of *IRE1a* and *IRE1b* have ribonuclease activity, we used an in vitro assay by using a 125b piece of RNA containing the kissing loop structure from *bZIP60* mRNA as substrate. As enzyme we used his-tagged, C-terminal components of IRE1a and IRE1b (HIS-cIRE1a and HIS-cIRE1b) synthesized in *Escherichia coli* and partially purified on a nickel column. Both

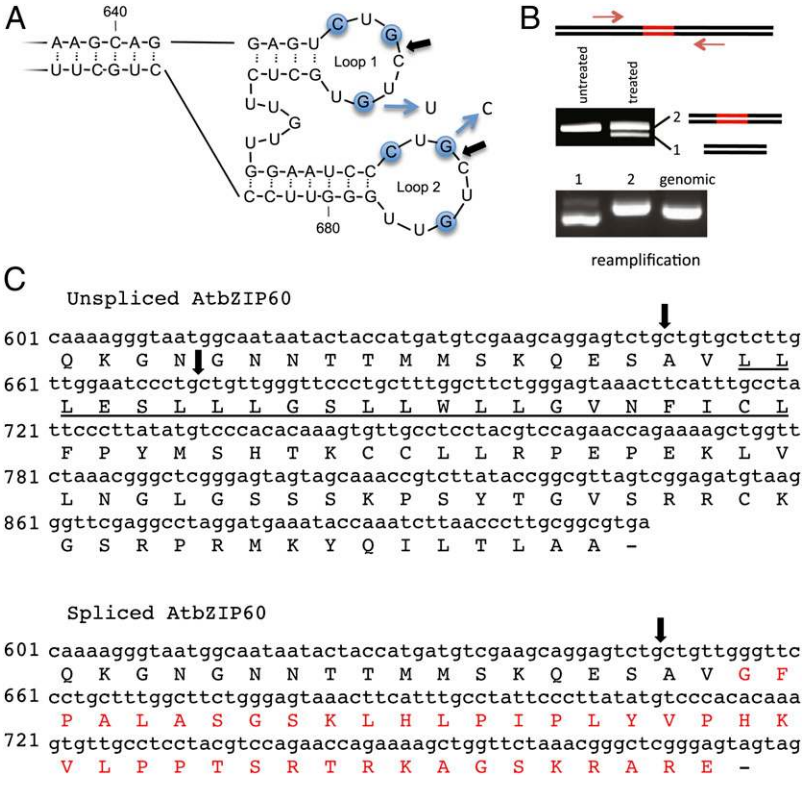

Fig. 1. Twin hairpin loop structure at splicing site in *bZIP60* mRNA. (*A*) Each of the two loops contains three conserved bases (highlighted). Solid block arrows indicate predicted cleavage sites. (Equivalent cleavage sites indicated by open block arrows.) Base substitution mutations are indicated with blue arrows. For constructs with a single point mutation (1PM), the G at nucleotide position 672 in loop 2 has been substituted by a C. This base substitution is not a coding change for *bZIP60* mRNA. Constructs with two point mutations (2PM) involve the base substitution in loop 2 and another one in loop 1 in which the G at nucleotide position 652 has been substituted by a U. The second base substitution changes the coding capacity of *bZIP60* mRNA; however, the change is a conservative one, exchanging a hydrophobic amino acid for another, a V to a L. (*B*) Splicing assay using primers immediately flanking splice site (*Upper*). Electrophoretic gel band pattern of RT-PCR products from RNA sample taken from untreated seedlings or seedlings treated for 2 h with 2 μg/mL tunicamycin. Interpretation of the various RT-PCR products (labeled 1–2) based on reamplication of cDNA from individual bands (*Lower*). (*C*) Partial sequence of cDNA derived from unspliced and spliced forms of *AtbZIP60* mRNA shown in *B*. Arrows indicate splice sites inferred from the sequence of the spliced mRNA. Underlined segment of the amino acid sequence derived from the unspliced form is a predicted transmembrane domain. Amino acid sequence in red predicted from the spliced RNA form represents differences in the sequence predicted from the unspliced form.

HIS-cIRE1a and HIS-cIRE1b containing the putative kinase and ribonuclease domains were active in vitro producing a series of discrete RNA fragments (Fig. S3). The fragment patterns produced by the two enzymes, HIS-cIRE1a and HIS-cIRE1b, were similar although the 58/55 fragment was recovered less frequently among the HIS-cAtIRE1a products. Nonetheless, the fragment pattern for HIS-cAtIRE1b, in particular, was consistent with predictions for cuts in the two loops (loop 1 and 2) as shown in Fig. 1*A*.

According to the *Arabidopsis* eFP browser (www.bar.utoronto.ca/efp/cgi-bin/efpWeb.cgi), both *Arabidopsis IRE1* genes are expressed at low levels. *IRE1b* is more generally expressed throughout the plant, while *IRE1*a is more locally expressed in embryos and seeds (17, 18). The activity capable of splicing *bZIP60* mRNA did not appear to be localized to a specific region of the seedling because splicing activity and *BIP3* induction were observed following 2 h of DTT treatment in seedling shoots, hypocotyls and roots (Fig. S4). T-DNA insertion mutations are available for both *IRE1* genes, so the splicing reactions in the mutants were tested. The *IRE1*a (*ire1-2-2*) mutation is an insertion in the third exon and is a null mutant, in that full-length transcripts were not detectable in the mutant (Fig. S5*A*). Homozygous *ire1a* mutant seedlings were subjected to DTT treatment, but *bZIP60* mRNA splicing appeared unaffected (Fig. 2*B*). The *ire1b* mutation is a T-DNA insertion in the penultimate (fourth) intron, and no full-length *IRE1*b transcripts were detectable (Fig. S5*B*). When homozygous *ire1b* mutants were subjected to ER stress agents, splicing of *bZIP60* mRNA was much reduced (Fig. 2*B*). Thus, *Arabidopsis IRE1*b is necessary for normal levels of *bZIP60* mRNA splicing in stressed seedlings, but *IRE1a* alone is not.

The excision of the 23b segment in the splicing of *bZIP60* RNA creates a frame shift, which results in the expression of downstream sequences in a different reading frame (Fig. 1*C*). The unspliced *bZIP60* RNA (bZIP60(u)) is predicted to encode a bZIP transcription factor with a transmembrane domain (TMD) in the C-terminal third of the protein (Fig. 2*C*). Splicing removes the TMD and alters the amino acid sequence further downstream. To determine whether splicing alters the subcellular localization of bZIP60, cDNAs representing the spliced and unspliced forms of bZIP60 were linked to YFP and transiently expressed in tobacco BY-2 cell protoplasts (Fig. 2*D*). Unspliced bZIP60-YFP is colocalized in the cytoplasm with an ER marker, whereas the spliced form is located in the nucleus.

bZIP60 Function Requires IRE1b-Catalyzed Splicing of *bZIP60* mRNA. To show that splicing of mRNA is required for bZIP60 function, base substitution mutations were created in the conserved bases of the paired loops of *bZIP60* mRNA (Fig. 1*A*). In the single point mutant (1PM), the G at nucleotide position 672 in loop 2 was substituted for a C. This base substitution did not represent a coding change for *bZIP60* mRNA. Constructs with two point mutations (2PM) involve the aforementioned base substitution in loop 2 and another one in loop 1 in which the G at nucleotide position 652 was substituted by U. The second base substitution represented a coding change for *bZIP60* mRNA, however, the change was a conservative one, exchanging a hydrophobic amino acid for another, a V to L.

The RNA splicing assay was carried out in the background of a T-DNA mutant (*bzip60-1*) with an insertion near the start codon (ATG) in *bZIP60* mRNA. The mutation reduced the background of endogenous *bZIP60* mRNA splicing in response to DTT treatment (Fig. 3*A*, compare lanes 1 and 2 with 3 and 4) to permit us to monitor the splicing of mRNA derived from the *bZIP60* transgenes. Splicing was observed in the mRNA derived from a nonmutant (0PM) cDNA construct of *bZIP60* (myc-bZIP60) in the *bzip60-1* background (Fig. 3*A*, lanes 5–8). Splicing did not occur in RNA derived from a full-length cDNA construct of *bZIP60* (myc-bZIP60) with one (1PM) or two point mutations (2PM, Fig. 3*A*, lanes 9–16). The level of RNA splicing in the mutants was comparable with the background of endogenous *bZIP60* splicing in *bzip60*-1 (Fig. 3*A*, lanes 3 and 4).

To confirm that the lack of spliced *bZIP60* mRNA derived from point mutants was not due to the absence of unspliced

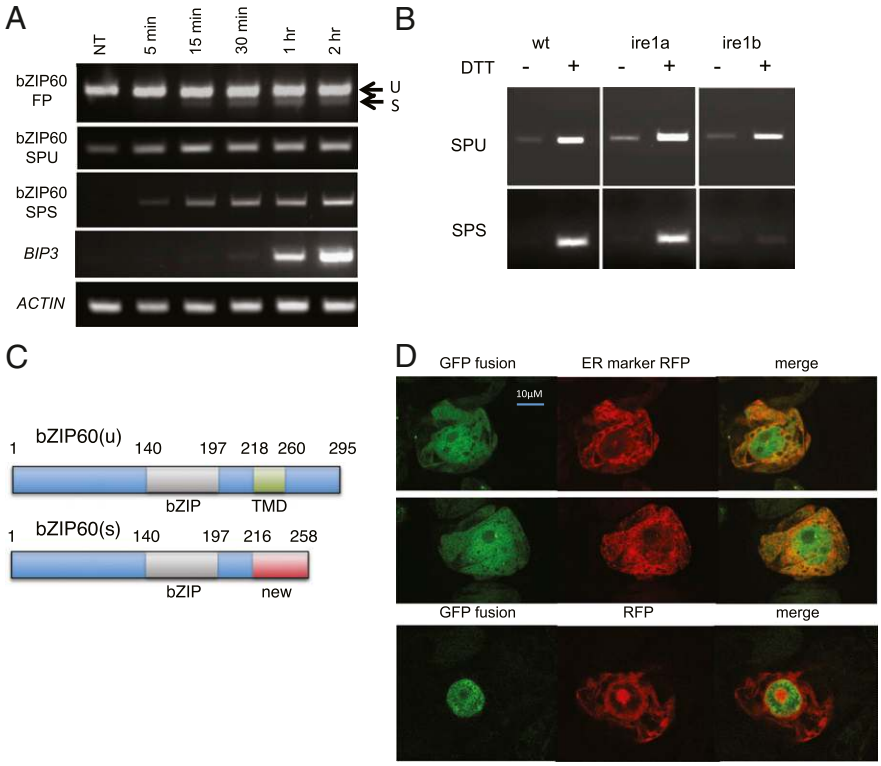

Fig. 2. Induction of *bZIP60* splicing by treatment with DTT. (*A*) Seedlings were transferred to liquid LS medium containing 2 mM DTT and incubated for the times indicated. RNA samples were analyzed for the presence of unspliced (U) and spliced (S) *bZIP60* mRNA by RT-PCR using the flanking primers (FP) assay or the specific primers assay using primers for unspliced *bZIP60* mRNA (SPU) or for spliced mRNA (SPS). Amplification with primers for actin mRNA was used as a control. (*B*) Effects of T-DNA mutations in IRE1a and IRE1b on splicing of *bZIP60* mRNA in seedlings. Seedlings were treated with 2 mM DTT and RNA was extracted 2 h later. *bZIP60* mRNA splicing was analyzed by SPU and SPS assays for the presence of unspliced and spliced RNA forms, respectively. (*C*) Diagrams illustrating the predicted structure of proteins derived from the unspliced and the spliced forms of *bZIP60* mRNAs. (*D*) Localization of bZIP60 proteins derived from unspliced (*Top* and *Middle*) and spliced mRNAs (*Bottom*). Constructs encoding GFP-tagged forms of bZIP60 were introduced by biolistics into tobacco BY-2 cells. RFP-HDEL was used as an ER marker, and RFP alone was used to mark both nuclei and cytoplasm.

bZIP60 mRNA, the transgenics were tested for presence of *bZIP60* mRNA. Endogenous *bZIP60* gene expression was up-regulated somewhat after DTT treatment (Fig. S6, lanes 1–2); however, *bZIP60* expression was undetectable with or without DTT treatment in the *bZIP60* T-DNA mutant (*bzip60-1*; Fig. S6, lanes 3 and 4). Full-length *bZIP60* mRNA was detected in all of the transgenics, roughly at levels comparable with endogenous RNA levels in wild type (Fig. S6, lanes 5–16). Expression of the *bZIP60* transgenes was relatively unaffected by stress treatment, although a slight upswing in expression after DTT treatment was noted in the 0PM sample #2 (Fig. S6, lanes 5 and 6). Hence, we can conclude that the lack of spliced forms in the point mutants is not due to the absence of mRNA derived from the transgenes and that the single or double point mutations in the conserved bases of the paired loops interfere with *bZIP60* mRNA splicing.

Equipped with mutations with defects in RNA splicing, we could address whether mRNA splicing is required to confer functionality on bZIP60. We observed that *BIP3* induction in response to DTT treatment was significantly reduced in the *bzip60-1* and *bzip60-2* mutant (a T-DNA line with an insertion near the splicing site in *bZIP60*) (Fig. 3*B*, lanes 3–6) compared with wild type (Fig. 3*B*, lanes 1 and 2). We also found that *BIP3* induction in response to DTT treatment largely depended on *IRE1b* (Fig. 3*B*, lane 8). Thus, *BIP3* up-regulation in response to ER stress substantially depends on *bZIP60* and *IRE1b*.

To determine whether the function of bZIP60 specifically depends on the splicing of its mRNA, *BIP3* expression supported by various *bZIP60* constructs was monitored in a *bzip60-1* background. As before with *bzip60-2*, *bip60-1* showed only modest up-regulation of *BIP3* expression in comparison with wild type (Fig. 3*C*, lanes 1–4). It was found that the nonmutant *bZIP60* construct complemented *bip60-1* by restoring full induction of *BIP3* expression in response to DTT treatment (Fig. 3*C*, lanes 5–8). However, the *bZIP60* constructs with point mutations in the conserved bases of the paired RNA loops did not support *BIP3* induction (Fig. 3*C*, lanes 9–16). The lack of *BIP3* induction is evident even in the case of the single point mutation (1PM), which does not represent a codon change in the mRNA. Thus, we conclude that *bZIP60* mRNA splicing is necessary for the functionality of bZIP60.

Conditions for Expression of AtIRE1 Activity. *Arabidopsis bZIP60* mRNA splicing can be induced in the laboratory by agents that interfere with protein folding, such as TM and DTT, but what natural environmental conditions elicit the response? We tested a variety of conditions and found using both the FP and SP assays that heat stress was most effective in eliciting *bZIP60* mRNA splicing. Exposure of seedlings to 42 °C for 30 min was sufficient to elicit the splicing response (Fig. 4*A*). Other conditions tested such as salt stress, hypoxia, and nutrient stress (nitrogen deprivation) did not generate this response (Fig. S7).

Heat treatment at 42 °C did not immediately lead to *BIP3* induction. However, if heat-treated seedlings were allowed to recover for 2 h at room temperature, then bZIP60-dependent *BIP3* induction was observed (Fig. S8*A*). *BIP3* expression was induced and modest amounts of *bZIP60* mRNA were spliced when seedlings were heat treated at a lower temperature, 37 °C (Fig. S8*B*). We interpret the difference in response at the two different temperatures to mean that heat treatment at 42 °C may also inactivate processes necessary for the *BIP3* up-regulation, but these processes recover at room temperature before the levels of spliced *bZIP60* mRNA fall. Alternatively, *BIP3* induction may be outcompeted by the induction of heat shock genes at the higher temperature. In either case, the lack of *BIP3* induction immediately following heat treatment at 42 °C may explain why it has been reported that *BIP3* is not induced by heat treatment in other plants (27, 28).

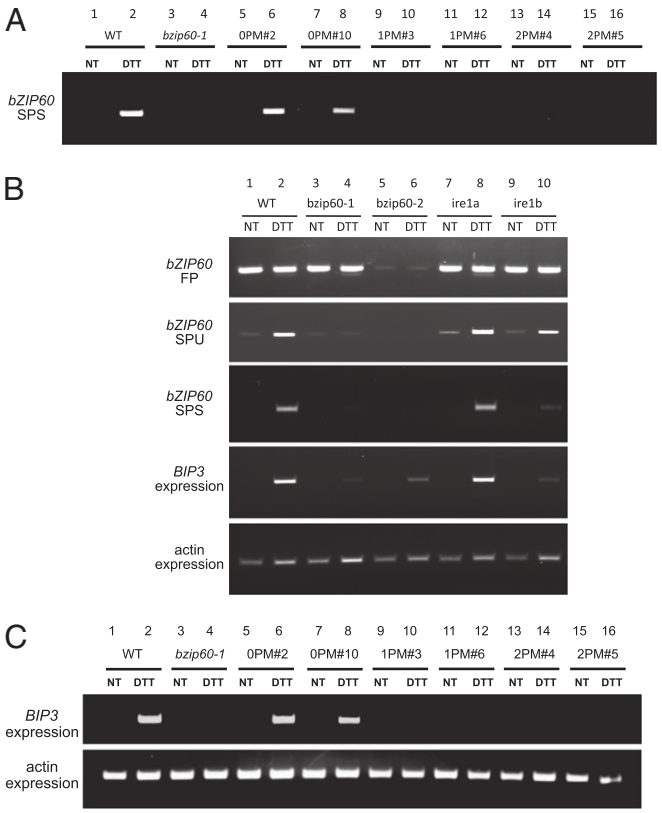

Fig. 3. In vivo splicing analysis of the transgenic plants. (*A*) Splicing of *bZIP60* mRNA was induced by treatment of seedlings with 2 mM DTT for 2 h. Splicing is demonstrated by use of the RT-PCR assay with splice specific primers (SPS assay). Lanes 1–4 show splicing of endogenous *bZIP60* mRNA. Lanes 5–16 show splicing of RNA derived from *bZIP60* transgenes in the background of *bzip60-1*. Transgenes bear no point mutations (0PM) or one or two point mutations (1PM or 2PM) in conserved bases in the splicing loops of *bZIP60* mRNA as illustrated in Fig. 1*A*. Two different transgenic lines were tested for each transgene. (*B*) BIP3 induction after treatment with 2 mM DTT for 2 h in *bzip60-2*, *ire1a*, and *ire1b* mutants. RNA analyzed by RT-PCR in which actin gene expression served as a control. (*C*) Complementation of *bzip60-1* by cDNA-encoding *bZIP60* mRNA without point mutations (0PM). Complementation is demonstrated by the support of *BIP3* expression as analyzed by using a RT-PCR assay. Lack of complementation by constructs bearing one or two point mutations (1PM or 2PM) in conserved bases in the splicing loops of *bZIP60* mRNA. Two different transgenic lines were tested for each transgene. Actin gene expression served as a control.

Discussion

bZIP60 was identified by Iwata and Koizumi (24) as a gene induced by UPR stress agents. They also demonstrated that a truncated form of bZIP60 expressed as a transgene could activate other UPR genes in the absence of stress. Because AtbZIP60 has features in common with ATF6 in mammalian cells, they assumed that *Arabidopsis* TF might be activated in the same way. Like ATF6, bZIP60 is a membrane-associated bZIP TF. ATF6 is activated by relocating from the ER to the Golgi apparatus in response to ER stress, and in the Golgi apparatus, ATF6 is proteolytically processed by S1P and S2P and released to the nucleus (29, 30). Recently, Iwata et al. (23) demonstrated that, in fact, bZIP60 is present in a full-length form associated with microsomes in untreated seedlings, and in response to stress, bZIP60 appears in a shorter form without its TMD and a substantial portion of bZIP60 population is found in the nucleus. The authors conclude that bZIP60 undergoes proteolytic processing in response to ER stress. However, unlike ATF6, bZIP60 does not have a canonical S1P site and still undergoes apparent proteolytic processing in an AtS1P

mutant. Iwata et al. (23) concluded that plants may have an undescribed mechanism for processing this stress-activated TF.

Since the discovery of bZIP60, two other stress-induced, membrane-associated TFs have been described in *Arabidopsis*, AtbZIP17, which responds to UPR agents, heat, and salt stress (20, 22) and AtbZIP28 that is activated by UPR agents and heat (21, 22, 31). Both of these factors are activated conventionally in a manner similar to the activation of ATF6. Both are membrane associated, have canonical S1P sites in their ER lumen-facing, C-terminal tails, and appear to rely on S1P and S2P for processing (29, 30). Thus, plants appear to have a conventional mechanism as described in mammalian cells for the processing of membrane-associated TFs.

The previous studies on bZIP60 (23, 24) present a dilemma for understanding how it is activated, and this study offers a solution. Activated forms of bZIP60 appear to be produced in a manner similar to Hac1 or XBP1 rather than like ATF6. *bZIP60* mRNA is spliced in response to stress, and the nature of the splice predicts a form of bZIP60 that lacks a transmembrane domain, but has acquired a putative nuclear targeting signal.

It is of interest to know how IRE1 in *Arabidopsis* is activated by environmental conditions. Credle et al. (2) determined the structure of luminal domain of IRE1 in yeast with the aim of understanding how it senses stress. The prevailing view had been that BiP dissociation from the luminal domain activates IRE1. BiP is thought to be a negative regulator of IRE1, and the accumulation of unfolded proteins in the ER is presumed to recruit BiP away from IRE1 allowing it to dimerize and oligomerize (32).

Credle et al. (2) proposed that unfolded proteins directly activate IRE1. They found that the core luminal domain of IRE1 forms an antiparallel β-sheet linking two IRE1 monomers "through their zippered central strands." Along either side of the β-sheet platform lies two α-helices forming the walls of a deep groove, which is thought to be able to bind the exposed loops of unfolded proteins tending to stabilize IRE1 dimers or to cross-link oligomers, thereby activating IRE1. In analyzing the structure of the human IRE1 luminal domain, Zhou et al. (13) also found that dimerization creates a similar groove, however, they concluded that the groove was too narrow to accommodate peptides and that peptide binding was not required for dimerization. Instead, they argued that BiP binding maintains IRE1 in an inactive monomeric state and that the imposition of ER stress promotes BiP release, leading to IRE1 dimerization (or oligomerization) and activation. Comparable studies on the structure and oligomerization of IRE1 will be needed to understand its activation in plants.

Materials and Methods

Lines and Growth Conditions. *Arabidopsis thaliana* ecotype Columbia-0 (Col-0) was used in this study, and the mutants *bzip60-1* (Col-0; SALK_050203), *bzip60-2* (Col-0, SAIL_283_B03, *ire1a* (Col-0; SALK_018112), and *ire1b* (Col-0; SAIL_238_F07) were obtained from Arabidopsis Biological Resource Center. Seeds were stratified at 4 °C for 3 d before germination. Unless indicated otherwise, plants were grown under continuous white light at 23–25 °C in soil or on Linsmaier Skoog (LS) medium (1× LS salts, 1% sucrose, 0.8% Agar). Agrobacterium-mediated transformation of *Arabidopsis* plants was carried out by the floral dip method (33). Agrobacterium strain GV3101 was used in all transformation experiments.

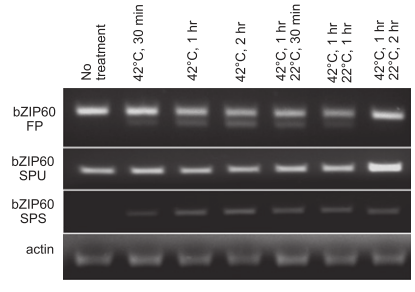

Fig. 4. Heat induction of *bZIP60* mRNA splicing. *Arabidopsis* seedlings were heat shocked at 42 °C for various times and, in the instances as indicated, were allowed to recover at room temperature (22 °C). RNA extracted from seedlings was analyzed by the FP assay for unspliced and forms of *bZIP60* mRNA or by the SPU assay for unspliced forms and the SPS assay for spliced forms of mRNA.

Stress Assays. To determine whether *bZIP60* mRNA is spliced in response to various stress agents or treatments, 2-wk-old wild-type Col-0 seedlings were grown on LS agar medium and then treated with liquid LS medium containing 10 μM ABA, 1 mM ethephon, or an equivalent volume of DMSO and incubated for the indicated times. In testing for salt stress, 8-d-old seedlings were grown on LS as described above and treated with liquid LS medium containing 100 mM NaCl or LS medium alone for the indicated time. To test for the effects of nitrogen limitation, plants were grown on soil and fertilized by using limiting nitrogen (0.5 mM KNO_3) or optimal nitrogen (10 mM KNO_3) solutions as described in Peng et al. (34). Leaf tissue was harvested 3 wk after germination.

In Vitro Ribonuclease Assay. The double loop region of *bZIP60* mRNA was synthesized and radiolabeled for use as a substrate in in vitro ribonuclease assays. A DNA template for in vitro RNA transcription was PCR-amplified by using primers T7bZIP-F and bZIP-8R. In addition to *bZIP60*-specific forward and reverse sequences, the primers respectively contain the T7 promoter used for in vitro transcription and a hairpin-forming sequence to prevent exonucleolytic degradation of the transcript (35). Using this template, the resulting RNA is expected to be 125 bases long and includes a 98-base sequence corresponding to the region surrounding the predicted splice sites in *bZIP60* mRNA (bases 624–721 of the transcript). The PCR product was gel-extracted and precipitated by using sodium acetate and ethanol. In vitro transcription was performed by using the MEGAshortscript kit (Ambion AM1354) following the manufacturer's instructions. Radioactive CTP was incorporated by using 4 μL of [α^{32}P]-CTP per reaction (Perkin-Elmer, 3,000 Ci/mmol, 10 mCi/mL). The reactions were incubated 4 h at 37 °C and treated with TURBO DNase. The product was denatured 5 min at 95 °C and run on a 0.4-mm-thick denaturing 10% polyacrylamide-urea gel for 2 h at 400 V. The gel was then transferred to a filter paper, wrapped in saran, and exposed to an X-ray film to localize the labeled RNA band, which was eluted overnight at 4 °C in equal volumes of acetate [0.3 M NaOAc, 10 mM $Mg(OAc)_2$] and phenol:chloroform:isoamylalcohol (25:24:1). The labeled RNA was purified two additional times, precipitated with ethanol, and resuspended in 20 μL of DEPC-treated H_2O before being used in the ribonuclease reaction.

Partial *IRE1a* and *IRE1b* sequences were amplified from wild-type *Arabidopsis* cDNA and cloned into pET28a by using EcoRI and NotI sites. These constructs allow the synthesis of recombinant proteins comprised of a N-terminal His tag fused to the C-terminal regions of IRE1 proteins starting after their predicted transmembrane domains and including the ribonuclease and kinase sites (respectively regions 345–841 and 375–881 of IRE1a and IRE1b protein sequences). pET42a vector was used for the expression of His-tagged GST. Recombinant protein were expressed in *E. coli* strain BL21 and induced by using 300 μM IPTG for 5 h 30 min at 30 °C. The recombinant proteins were purified by using Ni-NTA agarose beads (Qiagen), dialyzed overnight in 10 mM Hepes at pH 7.6, and quantified by using a Bradford assay (Bio-Rad).

The ribonuclease reaction procedure was modified from Back et al. (36). The 50-μL reaction mixture contained 7 μg of recombinant His-tagged protein (or an equivalent volume of 10 mM Hepes at pH 7.6), 50 mM KOAc, 10 mM $Mg(OAc)_2$, 1 mM DTT, 2 mM ATP, 40 U RNasin, and 2 μL of radio-labeled RNA substrate. The reaction was incubated at 37 °C for 1 h and stopped by using 5 volumes of stop buffer (100 mM NaOAc at pH 5.2, 2 mM EDTA, 0.2% SDS). The RNA products were extracted and precipitated with ethanol and resolved on a 12% polyacrylamide-urea gel.

Transient Expression in Tobacco Protoplasts. Constructs used in transient expression assays were pRTL2/RFP-MCS, pRTL2/RFP-HDEL, pRTL2ΔN/S/GFP-MCS, and pUC18-NcoI/GFP were kind gifts from S. Gidda (University of Guelph, Guelph, Ontario, Canada) and have been described in Shockey et al. (2006) (37). The construct used to express GFP-bZIP60(u) was obtained by inserting the unspliced version of bZIP60 coding sequence in pRTL2ΔN/S/GFP-MCS by using BamHI and XbaI sites. The construct used to express bZIP60(s)-GFP was obtained by inserting the spliced version of bZIP60 coding sequence in pUC18-NcoI/GFP by using the NcoI site. In addition to missing the 23-base intron, this version of bZIP60(s) is truncated at its 3′ end (starting from base 802 in the unspliced bZIP60 mRNA transcript) and, thus, does not contain

the early stop codon that would prevent the translation of the C-terminal fusion with GFP.

Tobacco (*Nicotiana tabacum* cv BY-2) suspension cell cultures were prepared for biolistic bombardment as described in Banjoko and Trelease (38). Transient cotransformations were performed by using 2 μg of each plasmid DNA with a biolistic particle delivery system (Bio-Rad Laboratories). After bombardment, cells were incubated for 6–24 h, then fixed in 4% (wt/vol) formaldehyde. Confocal Laser Scanning Microscopy images were acquired with a Leica DM RE (Leica Microsystems) microscope connected to a Leica TCS SP2 system by using a Leica 63× Plan Apochromat oil-immersion objective.

ACKNOWLEDGMENTS. This study was supported by National Science Foundation Grant IOS091907 (to S.H.H.) and the Plant Sciences Institute at Iowa State University.

1. Mittler R, Blumwald E (2010) Genetic engineering for modern agriculture: challenges and perspectives. *Annu Rev Plant Biol* 61:443–462.
2. Credle JJ, Finer-Moore JS, Papa FR, Stroud RM, Walter P (2005) On the mechanism of sensing unfolded protein in the endoplasmic reticulum. *Proc Natl Acad Sci USA* 102: 18773–18784.
3. Ron D, Walter P (2007) Signal integration in the endoplasmic reticulum unfolded protein response. *Nat Rev Mol Cell Biol* 8:519–529.
4. Bernales S, Papa FR, Walter P (2006) Intracellular signaling by the unfolded protein response. *Annu Rev Cell Dev Biol* 22:487–508.
5. Schröder M, Kaufman RJ (2005) The mammalian unfolded protein response. *Annu Rev Biochem* 74:739–789.
6. Mori K, Kawahara T, Yoshida H, Yanagi H, Yura T (1996) Signalling from endoplasmic reticulum to nucleus: transcription factor with a basic-leucine zipper motif is required for the unfolded protein-response pathway. *Genes Cells* 1:803–817.
7. Cox JS, Walter P (1996) A novel mechanism for regulating activity of a transcription factor that controls the unfolded protein response. *Cell* 87:391–404.
8. Rüegsegger U, Leber JH, Walter P (2001) Block of HAC1 mRNA translation by long-range base pairing is released by cytoplasmic splicing upon induction of the unfolded protein response. *Cell* 107:103–114.
9. Uemura A, Oku M, Mori K, Yoshida H (2009) Unconventional splicing of XBP1 mRNA occurs in the cytoplasm during the mammalian unfolded protein response. *J Cell Sci* 122:2877–2886.
10. Sidrauski C, Walter P (1997) The transmembrane kinase Ire1p is a site-specific endonuclease that initiates mRNA splicing in the unfolded protein response. *Cell* 90: 1031–1039.
11. Shamu CE, Walter P (1996) Oligomerization and phosphorylation of the Ire1p kinase during intracellular signaling from the endoplasmic reticulum to the nucleus. *EMBO J* 15:3028–3039.
12. Lee KP, et al. (2008) Structure of the dual enzyme Ire1 reveals the basis for catalysis and regulation in nonconventional RNA splicing. *Cell* 132:89–100.
13. Zhou J, et al. (2006) The crystal structure of human IRE1 luminal domain reveals a conserved dimerization interface required for activation of the unfolded protein response. *Proc Natl Acad Sci USA* 103:14343–14348.
14. Yoshida H, Matsui T, Yamamoto A, Okada T, Mori K (2001) XBP1 mRNA is induced by ATF6 and spliced by IRE1 in response to ER stress to produce a highly active transcription factor. *Cell* 107:881–891.
15. Yoshida H, Oku M, Suzuki M, Mori K (2006) pXBP1(U) encoded in XBP1 pre-mRNA negatively regulates unfolded protein response activator pXBP1(S) in mammalian ER stress response. *J Cell Biol* 172:565–575.
16. Lin JH, et al. (2007) IRE1 signaling affects cell fate during the unfolded protein response. *Science* 318:944–949.
17. Koizumi N, et al. (2001) Molecular characterization of two Arabidopsis Ire1 homologs, endoplasmic reticulum-located transmembrane protein kinases. *Plant Physiol* 127: 949–962.
18. Noh SJ, Kwon CS, Chung WI (2002) Characterization of two homologs of Ire1p, a kinase/endoribonuclease in yeast, in Arabidopsis thaliana. *Biochim Biophys Acta* 1575:130–134.
19. Martínez IM, Chrispeels MJ (2003) Genomic analysis of the unfolded protein response in Arabidopsis shows its connection to important cellular processes. *Plant Cell* 15: 561–576.
20. Liu JX, Srivastava R, Che P, Howell SH (2007) Salt stress responses in Arabidopsis utilize a signal transduction pathway related to endoplasmic reticulum stress signaling. *Plant J* 51:897–909.
21. Liu JX, Srivastava R, Che P, Howell SH (2007) An endoplasmic reticulum stress response in Arabidopsis is mediated by proteolytic processing and nuclear relocation of a membrane-associated transcription factor, bZIP28. *Plant Cell* 19:4111–4119.
22. Che P, et al. (2010) Signaling from the endoplasmic reticulum activates brassinosteroid signaling and promotes acclimation to stress in Arabidopsis. *Sci Signal* 3:ra69.
23. Iwata Y, Fedoroff NV, Koizumi N (2008) Arabidopsis bZIP60 is a proteolysis-activated transcription factor involved in the endoplasmic reticulum stress response. *Plant Cell* 20:3107–3121.
24. Iwata Y, Koizumi N (2005) An Arabidopsis transcription factor, AtbZIP60, regulates the endoplasmic reticulum stress response in a manner unique to plants. *Proc Natl Acad Sci USA* 102:5280–5285.
25. Oikawa D, Tokuda M, Hosoda A, Iwawaki T (2010) Identification of a consensus element recognized and cleaved by IRE1 alpha. *Nucleic Acids Res* 38:6265–6273.
26. Zuker M (2003) Mfold web server for nucleic acid folding and hybridization prediction. *Nucleic Acids Res* 31:3406–3415.
27. D'Amico L, et al. (1992) Bean homologs of the mammalian glucose-regulated proteins: induction by tunicamycin and interaction with newly synthesized seed storage proteins in the endoplasmic reticulum. *Plant J* 2:443–455.
28. Denecke J, Goldman MH, Demolder J, Seurinck J, Botterman J (1991) The tobacco luminal binding protein is encoded by a multigene family. *Plant Cell* 3:1025–1035.
29. Shen J, Prywes R (2004) Dependence of site-2 protease cleavage of ATF6 on prior site-1 protease digestion is determined by the size of the luminal domain of ATF6. *J Biol Chem* 279:43046–43051.
30. Ye J, et al. (2000) ER stress induces cleavage of membrane-bound ATF6 by the same proteases that process SREBPs. *Mol Cell* 6:1355–1364.
31. Gao H, Brandizzi F, Benning C, Larkin RM (2008) A membrane-tethered transcription factor defines a branch of the heat stress response in Arabidopsis thaliana. *Proc Natl Acad Sci USA* 105:16398–16403.
32. Liu CY, Schröder M, Kaufman RJ (2000) Ligand-independent dimerization activates the stress response kinases IRE1 and PERK in the lumen of the endoplasmic reticulum. *J Biol Chem* 275:24881–24885.
33. Bechtold N, Ellis J, Pelletier G (1993) In planta Agrobacterium-mediated gene transfer by infiltration of adult Arabidopsis thaliana plants. *C. R. Acad. Sci. Paris* 316: 1194–1199.
34. Peng M, Bi YM, Zhu T, Rothstein SJ (2007) Genome-wide analysis of Arabidopsis responsive transcriptome to nitrogen limitation and its regulation by the ubiquitin ligase gene NLA. *Plant Mol Biol* 65:775–797.
35. McLaren RS, Newbury SF, Dance GS, Causton HC, Higgins CF (1991) mRNA degradation by processive 3′-5′ exoribonucleases in vitro and the implications for prokaryotic mRNA decay in vivo. *J Mol Biol* 221:81–95.
36. Back SH, Schröder M, Lee K, Zhang K, Kaufman RJ (2005) ER stress signaling by regulated splicing: IRE1/HAC1/XBP1. *Methods* 35:395–416.
37. Shockey JM, et al. (2006) Tung tree DGAT1 and DGAT2 have nonredundant functions in triacylglycerol biosynthesis and are localized to different subdomains of the endoplasmic reticulum. *Plant Cell* 18:2294–2313.
38. Banjoko A, Trelease RN (1995) Development and application of an in vivo plant peroxisome import system. *Plant Physiol* 107:1201–1208.